Journal of Engineering Physics and Thermophysics, Vol. 77, No. 2, 2004

SCATTERING AND HEAT EXCHANGE OF DISPERSE IMPURITY PARTICLES IN TURBULENT NONISOTHERMAL GAS AND LOW-TEMPERATURE PLASMA JETS

K. N. Volkov and G. F. Gorshkov

UDC 532.529:536.24

This paper considers issues connected with the simulation of the motion and heat exchange of disperse impurity particles in nonisothermal gas and low-temperature plasma jets under the action of turbulent pulsations of the carrier flow. The influence of the outflow conditions, the initial parameters of the phases, and the conditions of particle injection into a jet flow on the laws of impurity scattering and heat exchange are investigated. The results of the numerical calculations are compared with the data obtained without taking into account the influence of turbulent pulsations on the particle motion.

Introduction. The intensification of the transfer properties of a medium in many technical devices (mixing chambers, gas generators, heat exchangers with a two-phase working medium) and the level of heat loads on the material being processed for the tasks of high-intensity technologies based on jet flows (for example, plasma processing of a disperse impurity and application of coatings) are largely due to the turbulent structure of jet flows and the presence of force-injected solid particles.

To describe and forecast the properties of such nonisothermal jet systems, the following approaches are used, as a rule: kinetic, continual, and discrete-trajectory ones. Practical realization of a particular approach is dictated, in the first place, by the applicability limits, prospects, the possibility of forecasting various characteristics of the flow, and the required calculation costs [1].

In modeling rarefied gas-disperse jet systems, where the interaction between particles and their influence on the carrier flow can be ignored, the application of the discrete-trajectory method of probe particles proves to be convenient. In this case, the equations describing the motion and heat-and-mass exchange of the dispersed phase are integrated along separate trajectories of individual particles in the known (preliminarily calculated) averaged field of carrier gas flow.

Depending on the model of interaction of a particle with a carrier medium, in particular, with the pulsation component of the turbulent flow rate, one distinguishes between the deterministic and the stochastic variant of the discrete-trajectory approach [1, 2].

In the deterministic variant, the position of the probe particle at the initial instant of time completely determines its further evolution on the only mechanical trajectory. In this case, the interaction of the particle with the turbulent moles was traditionally excluded from consideration, which is valid only for fairly inertial particles.

In the stochastic approach, the influence of turbulent pulsations on the impurity motion and heating is taken into account by introducing into the equation of motion a probe particle of random fluctuations of the carrier flow rate [2, 3]. The interaction of the particle with turbulent moles leads to a chaotic motion of the impurity, and the position of the particle at a given instant of time determines only the probability of its staying in an aggregate of possible states at each subsequent instant. To obtain a statistically reliable picture of the impurity motion, it is necessary to calculate a rather large number of probe particles.

The application of the stochastic variant of the discrete-trajectory approach for calculating nonisothermal jet systems makes it possible, in particular, to explain some abnormal phenomena observed in experiment, for example, such as particle pinching in the near-axis region of the jet (concentration of the disperse impurity in the near-axis zone

D. F. Ustinov Baltic State Technical University "Voenmekh," 1, 1st Krasnoarmeiskaya Str., St. Petersburg, 190005, Russia; email: kvolkov@uclan.ac.uk. Translated from Inzhenerno-Fizicheskii Zhurnal, Vol. 77, No. 2, pp. 51–57, March–April, 2004. Original article submitted September 17, 2003.

1062-0125/04/7702-0307

of the turbulent jet) as well as the scattering of particles (carrying out of particles beyond the jet boundaries) when they are injected longitudinally onto the nozzle exit section [4–6].

Comparison of the calculation results obtained from the point of view of the stochastic and deterministic models permits answering the question to what extent is the use of a particular approach justified, as well as how strong is the influence of carrier flow pulsations on the motion and heat-and-mass exchange of the impurity in turbulent gas and low-temperature plasma jets.

Modeling of the Carrier Phase. Let us consider the scattering and heat-and-mass exchange of spherical impurity particles in gas and low-temperature plasma jets (the superheating parameter $\vartheta_a = h_a/h_\infty$ is of the order of tens of orders of magnitude). The influence of the impurity on the carrier gas flow is ignored.

The statistical characteristics of turbulence for moderately heated jets ($\vartheta_a < 2$) are calculated by Reynolds equations written in the approximation of the nonisothermal boundary layer and the differential two-parameter k–ε1 Kolmogorov–Prandtl model of turbulence with Launder corrections [7].

For low-temperature plasma jets, the averaged flow of the carrier medium is modeled on the basis of the solution of V. V. Golubev-type relations for essentially nonisothermal jets with a changing composition [8]. The statistical characteristics of turbulence are determined within the framework of an approximate approach based on the analysis and application of semiempirical relations obtained as a result of the processing of data on the microstructure of isothermal and nonisothermal flows [9–14] in a wide range of change of the parameter ϑ_a = 1–5.3. Its essence is as follows.

1. Jet heating strongly influences the averaged field of the carrier gas:

a) the length of the initial portion decreases with increasing superheating of the jet according to [8];

b) the decay of the gas-dynamic parameters along the jet is more intensive than in the case of isothermal jets with an unchanged composition, and the degree of jet spread considerably increases.

2. Jet heating does not lead to considerable qualitative and quantitative changes in the microstructure of submerged jets [9–14];

a) the maximum value of the longitudinal component of the pulsation velocity in the mixing range is, as before, of the order of 15–17% of the gas velocity on the nozzle exit section;

b) the maximum of the longitudinal component of the pulsation velocity on the jet axis is situated at a distance equal to two distances of the initial portion of the jet and constitutes 13–15% of the corresponding value for unheated jets with an unchanged composition;

c) the radial distribution of velocity pulsations in the mixing range is characterized by a maximum shifting towards the jet axis with increasing distance from the nozzle exit section.

Let us give the basic semiempirical relations describing the distributions of the statistical characteristics of turbulence in a submerged jet. Align the x-axis of the cylindrical system of coordinates with the symmetry axis of the jet. Choose the origin of the coordinate system on the nozzle exit section.

The change in the turbulent velocity pulsations along the jet axis in generalized coordinates $u_l/u_{\max} = f(\xi)$ (here $\xi = x/x_s$) for jets with a natural level of initial turbulence on the nozzle exit section (1.5–2.5%) is universal and approximated by the dependence

$$\frac{u_l}{u_{\max}} = \begin{cases} 0.06 + 2\xi^{2.8} \exp(-1.35\xi) & \text{at } 0 < \xi \le 2, \\ 2.46\xi^{-1.3} & \text{at } 2 < \xi \le 5. \end{cases} \tag{1}$$

At Mach numbers on the nozzle exit section M_a = 0.15–0.5, the maximum value of turbulent pulsation is determined by the relation [13]

$$\frac{u_l}{U_a} = \begin{cases} 0.155 & \text{at } 0 \le x < 20, \\ 3.1/x & \text{at } 20 \le x \le 200. \end{cases} \tag{2}$$

For nonisothermal gas and plasma jets, the length of the initial portion is calculated by the formula [8]

$$x_s = 6.71 - 1.4 \log \vartheta_a. \tag{3}$$

The distribution of turbulent velocity pulsations in the mixing range obeys the dependence

$$\frac{u}{u_{\max}} = \frac{u_{\mathrm{m}}}{u_{\max}} \exp\left(-16.5\eta\right) + \frac{\partial U/\partial r}{(\partial U/\partial r)_{\max}}. \tag{4}$$

Here $(\partial U/\partial r)_{\max}$ is the maximum value of the mean velocity gradient; $\eta = (r - r_\delta)/\delta$ for the initial portion and $\eta = r/\delta$ for the main portion.

The kinetic energy of turbulent pulsations is calculated in the following way:

$$k = \frac{1}{2}\left(\langle u^2\rangle + \langle v^2\rangle + \langle w^2\rangle\right).$$

In so doing, it is taken into account that the transverse and circular components of the velocity pulsation constitute 70% of the longitudinal component.

Modeling of the Dispersed Phase. The equations describing the translatory motion of a spherical probe particle are of the form

$$\frac{d\mathbf{r}_{\mathrm{p}}}{dt} = \mathbf{V}_{\mathrm{p}}, \tag{5}$$

$$\frac{d\mathbf{V}_{\mathrm{p}}}{dt} = \frac{3C_{\mathrm{D}}\rho}{8\rho_{\mathrm{p}} r_{\mathrm{p}}} \left|\mathbf{V} - \mathbf{V}_{\mathrm{p}}\right| (\mathbf{V} - \mathbf{V}_{\mathrm{p}}). \tag{6}$$

The drag coefficient is given in the form

$$C_{\mathrm{D}} = \frac{24}{\mathrm{Re}_{\mathrm{p}}}\left(1 + 0.179\mathrm{Re}_{\mathrm{p}}^{0.5} + 0.013\mathrm{Re}_{\mathrm{p}}\right).$$

The Reynolds number in the relative motion of the particle and carrier gas is derived by the formula

$$\mathrm{Re}_{\mathrm{p}} = \frac{2r_{\mathrm{p}}\rho\left|\mathbf{V} - \mathbf{V}_{\mathrm{p}}\right|}{\mu}.$$

The equation of the temperature change describing the convective and radiative heat exchange between the spherical particle and the carrier gas is written in the form

$$\frac{dT_{\mathrm{p}}}{dt} = \frac{3}{c_{\mathrm{p}}\rho_{\mathrm{p}} r_{\mathrm{p}}}\left[\alpha\left(T - T_{\mathrm{p}}\right) - \psi\sigma T_{\mathrm{p}}^4\right]. \tag{7}$$

The heat-transfer coefficient is expressed in terms of the Nusselt number $\mathrm{Nu}_{\mathrm{p}} = 2r_{\mathrm{p}}\alpha/\lambda$, to calculate which one uses the dependence

$$\mathrm{Nu}_{\mathrm{p}} = 2 + 0.459\,\mathrm{Re}_{\mathrm{p}}^{0.55}\,\mathrm{Pr}^{0.33}.$$

Denote by $\zeta_{\mathrm{p}} = 1 - m_{\mathrm{p}}/m_{\mathrm{p0}}$ the relative molten mass of the particle. When the melting temperature is reached, the particle temperature $T_{\mathrm{p,m}}$ does not change, $dT_{\mathrm{p}}/dt = 0$, and the particle melting is described by the equation

$$\frac{d\zeta_{\mathrm{p}}}{dt} = \frac{3}{\Lambda\rho_{\mathrm{p}} r_{\mathrm{p}}}\left[\alpha\left(T - T_{\mathrm{p,m}}\right) - \psi\sigma T_{\mathrm{p,m}}^4\right]. \tag{8}$$

Thus, at $T_{\mathrm{p}} < T_{\mathrm{p,m}}$ and $T_{\mathrm{p}} > T_{\mathrm{p,m}}$ the particle temperature is calculated by Eq. (7) and at $T_{\mathrm{p}} = T_{\mathrm{p,m}}$ — by Eq. (8).

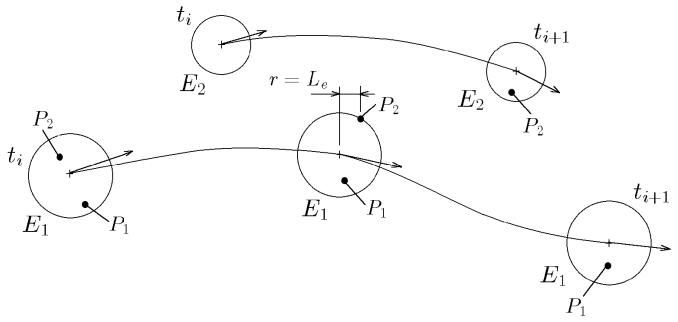

Fig. 1. Particle–turbulent mole interaction: P_1, P_2, particles; E_1, E_2, turbulent moles.

To calculate the impurity concentration, the continuity equation written in the Lagrangian coordinates

$$\frac{n_{\rm p}(\mathbf{r}_{\rm p0}, t)}{n_{\rm p}(\mathbf{r}_{\rm p0}, 0)} = \|w_{ij}\|^{-1}, \quad w_{ij} = \frac{\partial r_{{\rm p}i}(\mathbf{r}_{\rm p0}, t)}{\partial r_{{\rm p}j}(\mathbf{r}_{\rm p0}, 0)} \tag{9}$$

is used.

Equations (5)–(9) are integrated along the trajectory of an individual particle and require specification of only the initial conditions — coordinates, velocity, temperature and concentration of particles at time $t = 0$. The carrier-gas velocity and temperature are thereby random functions of the spatial coordinates and time.

Influence of Turbulence on the Impurity Motion. The influence of the jet-flow turbulence on the behavior of a disperse impurity is taken into account by introducing random fluctuations of the carrier-medium velocity into Eqs. (5)–(9). The gas velocity is given in the form of the sum of the averaged component and the random variable, which within the framework of the local-isotropic approximation is selected from the normal distribution law with a zero mathematical expectation and a standard deviation of $(2k/3)^{0.5}$.

The turbulence field is modeled by an aggregate of spherical vortices of different sizes, and the velocity fluctuation of interest is assumed to be unaltered inside a vortex during its lifetime. Let, at time t_i, particles P_1 ad P_2 be in vortex E_1, whose sizes are characterized by an integral scale of turbulence (Fig. 1). The gas mole, when moving, carries away the particles that have gotten into it. With regard for the relative motion of the vortex and particles at time t_{i+1}, three situations are possible: 1) the particles remain within the initial turbulent mole and move together with it (particle P_1, and $r < L_{\rm e}$ thereby); 2) the particles leave the initial mole (particle P_2, and $r > L_{\rm e}$ thereby); 3) the lifetime of the vortex expires and it loses its individuality ($t_{i+1} - t_i > \Theta_{\rm e}$), and the particles thereby get into a new turbulent mole and a new interaction process begins.

As soon as the particle leaves the vortex or the lifetime of the vortex expires, a new fluctuation is generated [2, 3]. The vortex lifetime and size, with which the fluctuation is associated, are determined by the local characteristics of the jet-flow turbulence. The turbulence characteristics are calculated by relations (1)–(4).

As a time criterion for the generation of a new fluctuation, the minimum from the lifetime of the vortex $\Theta_{\rm e}$ and the time of particle passage through the vortex $\Theta_{\rm c}$ is used, namely,

$$\Theta = \min\left\{\Theta_{\rm e}, \Theta_{\rm c}\right\} = \min\left\{\frac{L_{\rm e}}{\sqrt{2k/3}}, -\tau_v \ln\left(1 - \frac{L_{\rm e}}{\tau_v \left|\mathbf{V} - \mathbf{V}_{\rm p}\right|}\right)\right\}.$$

The dynamic relaxation time of the particle is calculated by the relation

$$\tau_v = \frac{8}{3}\frac{\rho}{\rho_{\rm p}}\frac{r_{\rm p}}{C_{\rm D}\left|\mathbf{V} - \mathbf{V}_{\rm p}\right|}.$$

As a spatial criterion, the integral scale of turbulence is used. In the cross sections of the jet, it is assumed to be constant and equal to the axial value. To calculate the scale of turbulence, we have obtained an empirical dependence of the form

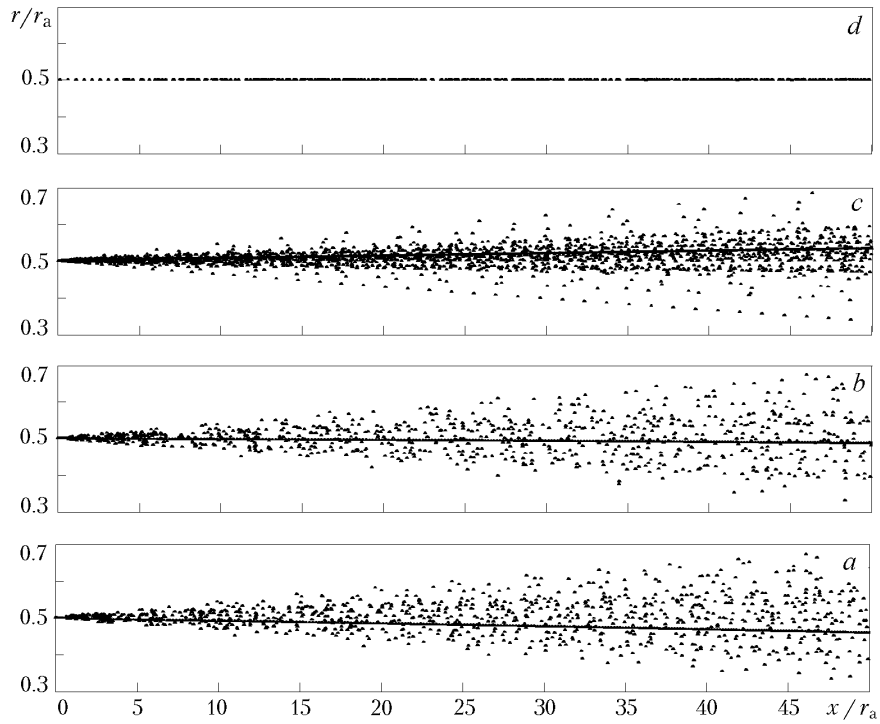

Fig. 2. Realizations of random particle trajectories (Y = 0.5). Influence of the particle size and blowing velocity: r_p = 10 μm (a, b), r_p = 50 μm (c, d) and $U_{p.a}$ = 0 m/sec (a, c), $U_{p.a}$ = 500 m/sec (b, d).

$$L_e = \begin{cases} 0.026x + 0.056 & \text{at } 0 \le x \le 13.5, \\ 0.009x + 0.28 & \text{at } 13.5 < x \le 40, \\ 0.016x & \text{at } 40 < x. \end{cases}$$

If $L_e > \tau_v |\mathbf{V} - \mathbf{V}_p|$, then the expression for Θ_c loses meaning. This means that the particle does not leave the vortex and remains within its limits as long as it exists. In so doing, the time criterion of the generation of a new velocity fluctuation is assumed to be equal to Θ_e.

Results of the Calculations and Discussion. To describe the behavior of an impurity in a turbulent jet on the basis of the stochastic model, it is necessary to calculate the trajectories of a large number of probe particles. In the calculations, from 1000 to 8000 trajectories of probe particles depending on their size were modeled. The integration step along each trajectory was restricted by the temporal and spatial scales of turbulence. A decrease in the particle size led to an increase in the number of realizations needed for obtaining a statistically reliable picture of the impurity motion as a result of the increased contribution of the particle interaction with vortices of ever decreasing sizes.

Some of the results of the numerical calculations of the aluminum oxide impurity scattering and heating in a submerged air plasma jet at a longitudinal blowing of particles onto the nozzle exit section are given in Figs. 2–5. The initial parameters of the gas and dispersed phases are as follows: r_a = 3 mm, U_a = 500 m/sec, T_a = 4700 K, $U_{p.a}$ = 0–500 m/sec, $T_{p.a}$ = 300 K, r_p = 5–50 μm. The thermophysical properties of the gas and particles are the reference ones (with allowance for the temperature dependence). As characteristic scales for variables with a length dimension, the radius of the nozzle outlet section is taken, and for variables with velocity and temperature dimensions the gas velocity and temperature on the nozzle exit section are taken.

The nonisothermality of the flow leads to a more intensive, compared to the incompressible flow, decay of the gas-dynamic, thermal, and pulsation parameters throughout the spreading portion of submerged gas and plasma jets. However, in this case, too, the kinetic energy grows downstream with its subsequent fall and a shift of the maximum values towards the jet axis.

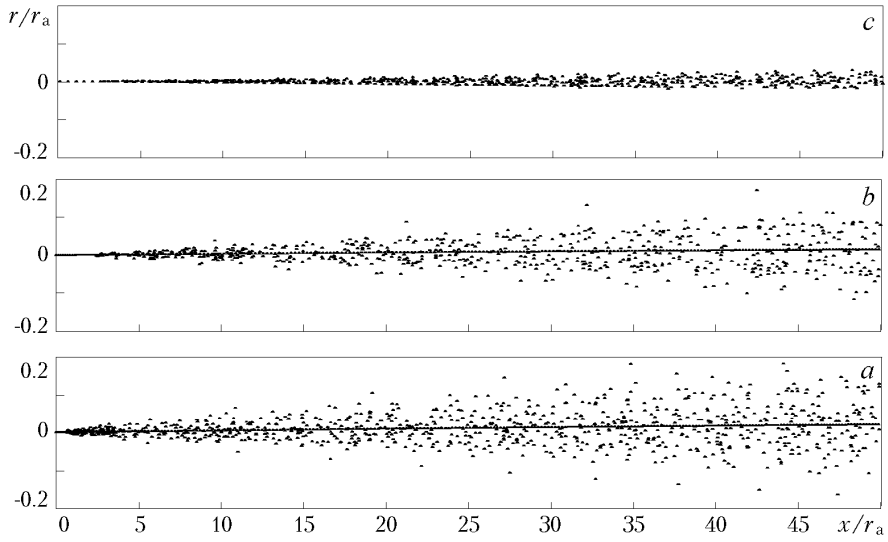

Fig. 3. Realizations of random particle trajectories along the jet axis (Y = 0) at r_p = 10 μm. Influence of the blowing velocity: $U_{p.a}$ = 0 (a); 125 (b); 500 m/sec (c).

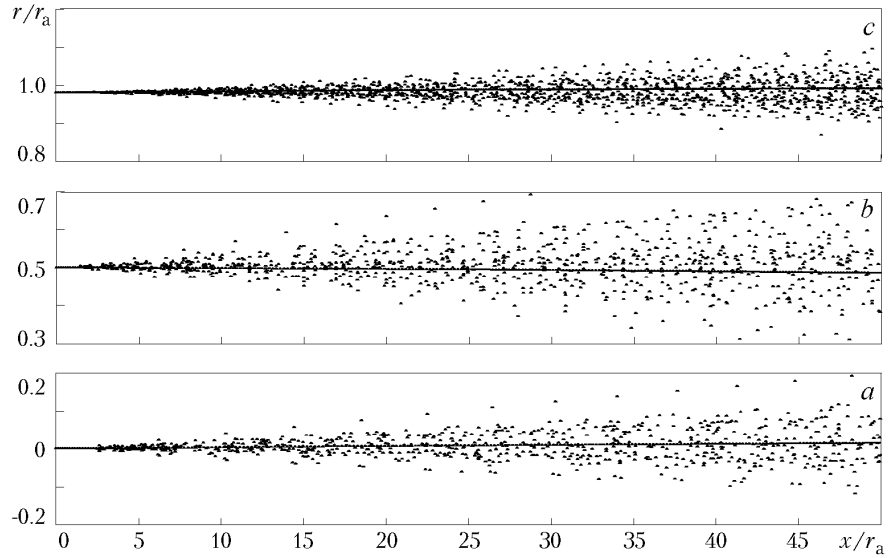

Fig. 4. Realizations of random particle trajectories at r_p = 10 μm at $U_{p.a}$ = 125 m/sec. Influence of the place of blowing particles onto the nozzle exit section: Y = 0 (a); 0.5 (b); 1 (c).

The results pertaining to the impurity scattering by the spreading portion of the jet depending on the size of the particles and the place (coordinate Y) and velocity of their blowing onto the nozzle exit section are given in Figs. 2–4. Solid lines correspond to the results averaged over the ensemble of realizations.

In modeling the impurity motion within the framework of the deterministic approach, the trajectories of heavy particles are lines parallel to the symmetry axis of the jet (the transverse component of the jet flow rate does not appreciably influence the motion of heavy particles).

The stochastic model takes into account the interaction of particles with turbulent moles. In so doing, the inhomogeneity of the turbulence field of the gas phase with the presence of a substantial minimum of kinetic energy in the near-axis region of the jet for particles of small fractions ($r_p \sim 10$ μm) leads to the appearance of a turbulent migration of a particle (turbophoretic force) directed towards a decrease in the pulsation energy of the gas — towards

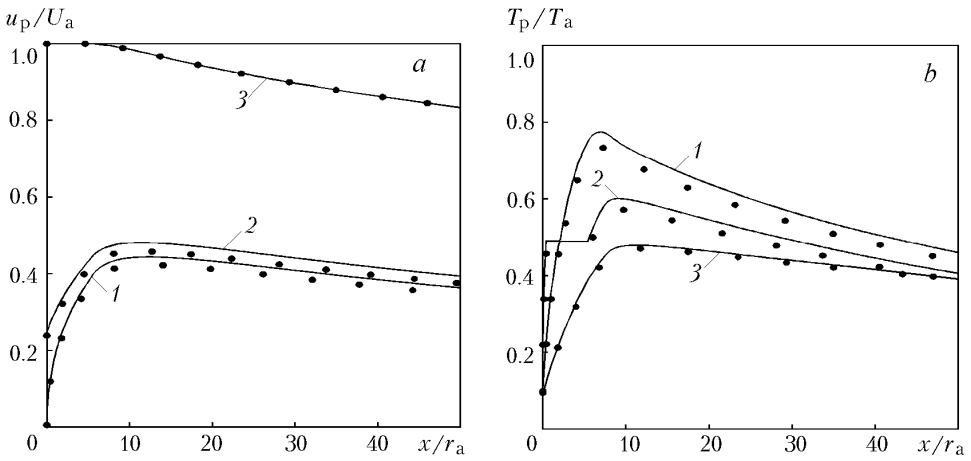

Fig. 5. Velocity (a) and temperature (b) of particles along the jet axis (Y = 0 and r_p = 10 μm): $U_{p.a}$ = 0 (1); 125 (2), and 500 m/sec (3).

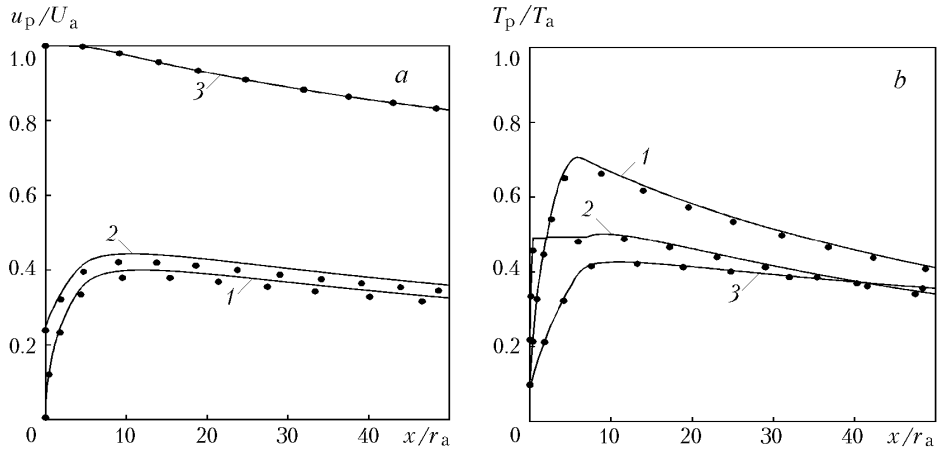

Fig. 6. Velocity (a) and temperature (b) of particles along the jet axis (Y = 0.5 and r_p = 10 μm): $U_{p.a}$ = 0 (1); 125 (2), and 500 m/sec (3).

the jet axis (Fig. 2a). In the main segment of the jet the kinetic energy gradients of turbulence near the jet axis are small; therefore, the influence of the turbophoresis decreases.

For particles of large fractions ($r_p \sim 50$ μm), the velocity pulsations have no appreciable effect on the impurity motion throughout the spreading portion of the jet by virtue of the inertia of such particles. However, in this case there is also a weak migration of particles directed towards a decrease in the gas pulsation energy (Fig. 2c).

A decrease in the initial rate of particle motion (from U_a to 0) leads to a stronger scattering of the impurity (Fig. 3). Such a behavior of the impurity is due to the fact that particles with an initial rate of motion lower than the flow rate move for a longer time in the region with the maximum level of turbulent pulsations (in the zone of the initial portion of the jet). A change in the position of the point Y at which particles are blown onto the nozzle exit section shows that the strongest scattering of the impurity takes place when particles are supplied in the range of coordinates $0 \le Y \le 0.5$, and the weakest scattering — at Y = 1 (Fig. 4).

As one moves away from the nozzle exit section, not only migration of the impurity towards the jet axis but also its scattering into the peripheral zone of the jet takes place. In the far region of the jet, where the migration transfer is small, the disperse impurity scattering is largely determined by the turbulent diffusion processes.

The influence of turbulent velocity pulsations on the motion of the particle begins to show up when it gets into the turbulent region of the jet. The dynamic behavior of the particle in the turbulent flow is determined by a parameter equal to the ratio between the dynamic relaxation time of the particle and the Euler time integral scale of turbulence Θ_e. A change in Θ_e due to the jet spread causes a nonmonotonic change in the degree of involvement of the

particle in the pulsating gas flow. The influence of particle inertia on its scattering in the cross section of the jet manifests itself indefinitively, since particles with a different mass execute motion in regions with a different turbulence intensity.

The dynamic and thermal characteristics of the particle along the jet axis averaged over the ensemble of realizations are given in Figs. 5 and 6. Points correspond to the results obtained from the viewpoint of the deterministic model (without taking into account the particle interaction with the pulsating structure of the flow). If, in the initial cross section of the jet, $U_{p.a} = U_a$, then subsequently the velocity of particles, because of their inertia, does not manage to decrease along the jet length as rapidly as the carrier flow rate. In the main segment of the jet, the particle temperature exceeds the temperature of the carrier phase. Because of their higher thermal inertia, the particles cool down more slowly than the gas. The character of the above distributions in nonisothermal jets depends on the initial conditions and is determined by the diffusion and migration transfer mechanism.

Analysis of the data obtained shows that at a given initial disbalance of flow rates ($U_a \neq U_{p.a}$; curves 1 and 2 in Figs. 5a and 6a) an increase in the particle size from $r_p = 10$ to $r_p = 50$ μm leads to a worsening of its melting (see, for example, curves 2 in Figs. 5 and 6). It should be noted that the rise of the particle temperature curve T_p after it has gotten onto the "shelf" corresponding to the melting temperature of the aluminum oxide particle $T_{p.m} = 0.484$ points to the particle's complete melting (its phase state is liquid).

An increase in the initial velocity of the particle being blown also worsens its heating. At high initial velocities of blowing (equilibrium flow $U_p = U_{p.a}$, curves 3 in Figs. 5 and 6) for a given fractional composition of the impurity, the particle temperature does not even reach its melting temperature.

The account of turbulent pulsations leads to the fact that not all particles blown from the nozzle exit section turn out to be melted (with their equal initial size). Part of them thereby either do not melt at all or their melting radius undergoes a nonmonotonic change over the course of time.

The dynamic state of the particle along the jet axis from distances $x > 10$ is characterized by a practically uniform velocity.

CONCLUSIONS

Simulation of the processes of turbulent momentum and heat transfer in nonisothermal dispersion gas and low-temperature plasma jets within the framework of the stochastic variant of the discrete-trajectory approach shows that pulsations of the jet flow rate strongly influence the impurity scattering and heat-and-mass exchange, and the model constructed leads to satisfactory results agreeing with the known data of numerical and physical experiments. The outflow conditions and the conditions of injection of particles into a jet flow largely determine the character of the motion, heating, and scattering of a disperse impurity due to the migration transfer mechanism.

NOTATION

c_p, specific heat capacity of a particle, J/(kg·K); f, functional dependence; h, enthalpy, J/kg; k, kinetic energy of turbulent pulsations, m^2/sec^2; m, mass, kg; n, concentration, m^{-3}; r, radial coordinate, m; $\mathbf{r}$, radius vector, m; r_a, radius of the outlet nozzle section, m; r_p, particle radius, m; t, time, sec; u, v, and w, rms value of the longitudinal, radial, and circular components of pulsation velocity, m/sec; x, longitudinal coordinate, m; C_D, drag coefficient; L, spatial scale, m; M, Nu, Pr, and Re, Mach, Nusselt, Prandtl, and Reynolds numbers; T, temperature, K; U, longitudinal averaged velocity, m/sec; $\mathbf{V}$, velocity vector, m/sec; Y, coordinate of particle injection onto the nozzle exit section; α, heat-transfer coefficient, $W/(m^2 \cdot K)$; δ, mixing-range thickness, m; ε, dissipation rate of kinetic energy of turbulence, m^2/sec^3; ζ_p, relative molten particle mass; ϑ, superheating parameter; λ, heat-conductivity coefficient, W/(m·K); μ, dynamic viscosity, kg/(m·sec); ξ, η, self-simulated variables; ρ, density, kg/m^3; σ, Stefan–Boltzmann constant, $W/(m^2 \cdot K^4)$; τ_v, particle relaxation time, sec; ψ, emissivity factor of the particle surface; Θ, characteristic time scale, sec; Λ, specific melting heat, J/kg; <...>, time averaging. Subscripts: a, nozzle exit section; c, time of particle–vortex interaction; e, turbulent vortex; i, j, tensor indices; l, jet axis; m, melting point; max, maximum; p, particle; s, starting segment of the jet; v, velocity characteristics; 0, zero time.

REFERENCES

1. C. T. Crowe, T. R. Troutt, and J. N. Chung, Numerical models for two-phase turbulent flows, *Ann. Rev. Fluid Mech.*, **28**, 11–43 (1996).
2. A. D. Gosman and E. Ioannides, Aspects of computer simulation of liquid-fueled combustors, *AIAA Paper*, No. 81-0323 (1981).
3. K. N. Volkov and V. N. Emel'yanov, Stochastic model of motion of a condensed particle in a channel with permeable walls, *Matem. Modelir.*, **11**, No. 3, 105–111 (1999).
4. T. A. Girshovich, A. I. Kartushinskii, M. K. Laats, et al., Experimental investigation of a turbulent jet carrying heavy impurities, *Izv. Akad. Nauk SSSR, Mekh. Zhidk. Gaza*, No. 5, 26–31 (1981).
5. M. K. Laats, On the transfer of a heavy impurity by a turbulent flow, in: *Turbulent Two-Phase Flows* [in Russian], Tallinn (1982), pp. 62–71.
6. S. I. Navoznov, A. A. Pavel'ev, A. S. Mul'gi, and M. K. Laats, Influence of initial sliding on the impurity scattering in a two-phase jet, in: *Turbulent Two-Phase Flows* [in Russian], Tallinn (1979), pp. 149–157.
7. K. N. Volkov and G. F. Gorshkov, Simulation of the processes of turbulent transfer of momentum and heat in nonisothermal disperse jets, in: *Proc. IV Minsk Int. Forum "Heat and Mass Transfer–MIF-2000"* [in Russian], May 22–26, 2000, Vol. 6, Minsk (2000), pp. 203–212.
8. G. F. Gorshkov, Propagation of cocurrent nonisothermal gas and plasma jets of variable composition, in: *Dynamics of Inhomogeneous and Compressible Media* [in Russian], LGU, Leningrad (1984), pp. 164–175.
9. G. F. Gorshkov, V. S. Komarov, and V. S. Terpigor'ev, Some measurement data on the mean and longitudinal components of velocity fluctuation in the initial fragment of the axisymmetric subsonic jet, in: *Hydrodynamics and Elasticity Theory* [in Russian], Issue 16, DGU, Dnepropetrovsk (1973), pp. 46–52.
10. K. N. Volkov and G. F. Gorshkov, Heat exchange of dispersed impurity particles in turbulent gas and plasma jets, in: *Proc. IIIrd Russ. Natl. Conf. on Heat Transfer* [in Russian], October 22–25, 2002, Moscow, Vol. 5, Moscow (2002), pp. 187–190.
11. V. I. Kukes and L. P. Yarin, Study of turbulent heat transfer in nonisothermal jets, in: *Heat and Mass Transfer-V* [in Russian], Vol. 1, ITMO AN BSSR, Minsk (1976), pp. 167–171.
12. J. C. Lau, Mach number and temperature effects of jets, *AIAA J.*, **18**, No. 6, 609–610 (1980).
13. J. C. Lau, Effects of exit Mach number and temperature on mean-flow and turbulence characteristics in round jets, *J. Fluid Mech.*, **105**, 193–218 (1981).
14. B. P. Ustimenko, V. N. Zmeikov, A. A. Shishkin, and B. O. Rivin, On the effect of the degree of flow nonisothermality on the jet flow characteristics, in: *Turbulent Jet Flows* [in Russian], Pt. 1, ITEF AN ESSR, Tallinn (1985), pp. 21–26.